

Relativistic optimized potential method for open-shell systems

D. Ködderitzsch,¹ H. Ebert,¹ and E. Engel²

¹*Department Chemie und Biochemie, Physikalische Chemie, Ludwig-Maximilians-Universität München, Butenandtstraße 11, D-81377 München, Germany*

²*Institut für Theoretische Physik, J. W. Goethe-Universität Frankfurt, Max-von-Laue-Straße 1, D-60438 Frankfurt/Main, Germany*
(Received 19 September 2007; published 2 January 2008)

A formulation of the relativistic optimized potential method (ROPM) within spin-density functional theory is presented. Various forms of the corresponding ROPM equations are given that allow to determine the spin-averaged and spin-dependent exchange-correlation fields. For a numerical basis-set-free implementation of the scheme, we use the exact exchange. Results are presented for a number of free atoms that demonstrate the implication of the fully relativistic approach as well as the impact of making use of the Krieger-Li-Iafarate approximation. The application of the present ROPM scheme to solids is briefly discussed.

DOI: [10.1103/PhysRevB.77.045101](https://doi.org/10.1103/PhysRevB.77.045101)

PACS number(s): 71.15.Mb, 31.15.E-, 31.30.J-, 32.10.Fn

I. INTRODUCTION

Density functional theory (DFT) is nowadays a widely used tool for calculating the electronic and magnetic properties of a vast spectrum of systems ranging from atoms and molecules to solids, from insulators to metals.^{1,2} Its tremendous success in treating the many-body problem is to a large part due to the virtue of the local (spin-) density approximation [L(S)DA] for the exchange-correlation functional.³ DFT functionals have evolved from using the density as basic variable to a second generation involving generalized gradient approximations (GGAs) and, finally, to the so-called third generation version which uses orbitals as ingredients to capture the physics of a broad range of systems.^{4–12} The latter approach turned out to be very fruitful as using orbital functionals in the so-called exact exchange approach cured some of the notorious problems of LDA and GGAs. In particular, this approach is self-interaction-free and the discontinuities of the functional derivative at integer electron numbers, which the exact exchange-correlation functional should have, are recovered (for an overview, see Ref. 6). Also, this method has successfully been used to describe long-range van-der-Waals interactions, which is not possible in a local density approach.^{10,13} Lastly, use of orbital functionals has opened a route for a systematic inclusion of correlations into DFT, once the exchange has been dealt with exactly.¹⁰

Using the exact exchange expression, recently several promising applications have demonstrated the versatility of the method.^{14–17} When exchange contributions dominate as compared to correlation, the exact exchange method should give reliable results. As long as the correlation contribution is not known, however, successes should be judged with care. Nevertheless, the formal development of orbital functional methods in the exact exchange approximation is of paramount importance on the route to more sophisticated orbital functionals.

Using orbital functionals requires the use of the optimized potential (OPM) method^{4,18–20} to calculate the effective potential (note that synonymously the term OEP is used in the literature). The foundations of this approach have been laid by Sharp and Horton²¹ and Talman and Shadwick,⁴ and were later developed further by several other authors. The natural

starting point was a nonrelativistic formulation which has later been extended to a spin-polarized²² and relativistic albeit non-spin-polarized form.^{10,19} Up to now no formulation and implementation of this method have been presented in a relativistic spin-polarized form. It should be mentioned that these methods require a much more involved analytical and numerical effort than LDA or GGAs.

In this paper, we formulate the equations and present exact numerical solutions of the relativistic OPM within spin-density functional theory (SDFT) for free atoms in the exact exchange approximation to the exchange-correlation functional. Our work is motivated by several aspects. First, a relativistic formulation will allow to make contact to current-density functional theory (CDFT),^{23,24} whose formulation naturally starts in a relativistic context. As CDFT is much more involved than standard DFT, a spin-polarized ROPM should be one step on the route to CDFT and will allow to carefully judge results obtained with it. CDFT in its local formulation and/or approximation nowadays is still not generally applicable because a suitable exchange-correlation functional in terms of the current is not available. Second, studying a spin-polarized relativistic formulation in which spin-orbit coupling effects are naturally included is a starting point for studying magnetic anisotropies in solids and analyzing the impact of relativistic effects in spectroscopy. Also, starting from a Dirac Hamiltonian where these effects are naturally included and no recourse to a perturbative treatment is needed is more elegant from a purists view. Third, an exact numerical (i.e., basis-set-free) solution of the ROPM evades any discussion about the choice of basis sets, cutoffs, etc. In our approach, we will avoid, in particular, the so-called sum over states approach to construct the Green's function. The limits of the sum over states approach can already be seen in a correlation treatment within the nonrelativistic OPM.²⁵ Finally, of course, relativistic effects play an important role in heavy atoms and are notoriously hard to handle within standard quantum chemical schemes.

In what follows, we will formulate different solution strategies and approximations for the ROPM equations to judge their use in the relativistic context. The conventional method^{4,18–20} which involves the inversion of response functions is a delicate matter. We will lay down the formalism and discuss several issues appearing in the relativistic do-

main. An important one is the construction of the so-called orthogonal Green's function which avoids the sum over states approach. Recently, it has been emphasized that the so-called orbital shifts^{6,26,27} lead to an elegant formulation of the OPM equations^{28,29} and lend themselves to a starting point for an iterative construction of the (R)OPM potentials,^{28,29} thereby avoiding the involved inversion procedure. In addition, this method allows to easily formulate the so-called Krieger-Li-Iafarate (KLI) approximation,³⁰ whose virtues we will study here.

The paper is organized as follows: in Sec. II, we derive the ROPM-SDFT equations and recast them in various forms. We give details on the construction of orbitals and response functions in the relativistic formulation and highlight several aspects which are of special importance for an implementation. We will also sketch the construction of the orthogonal Green's function (a detailed derivation and analysis of the latter will be given in Ref. 34). The next section will cover all numerical aspects of an implementation. In Sec. IV, we will present results obtained with various schemes and in different approximations, and discuss them. Finally, we give a brief summary.

II. THEORY

A. Derivation of the relativistic optimized potential method equations

Our starting point is the Dirac equation within relativistic Kohn-Sham (KS) SDFT³¹

$$\mathcal{H}_D \phi_k(\mathbf{r}) = \epsilon_k \phi_k(\mathbf{r}). \quad (1)$$

It is derived from the general KS Dirac scheme by applying a Gordon decomposition of the four current density into an orbital current and spin current density, respectively, and retaining only the coupling of spin to the magnetic field, thereby neglecting the orbital current contribution. The Hamiltonian (in atomic Rydberg units) is given as

$$\mathcal{H}_D = -ic\boldsymbol{\alpha} \cdot \nabla + \frac{c^2}{2}\boldsymbol{\beta} + V_{KS}(\mathbf{r}). \quad (2)$$

The index k comprises the set of quantum numbers which will be specified in Sec. II C. The Dirac and spin matrices α_i ,

β , and $\boldsymbol{\Sigma}$ have the usual meaning³¹⁻³³ and are given as ($i = x, y, z$)

$$\alpha_i = \begin{pmatrix} 0_2 & \sigma_i \\ \sigma_i & 0_2 \end{pmatrix}, \quad \beta = \begin{pmatrix} I_2 & 0_2 \\ 0_2 & -I_2 \end{pmatrix}, \quad \Sigma_i = \begin{pmatrix} \sigma_i & 0_2 \\ 0_2 & \sigma_i \end{pmatrix}. \quad (3)$$

The KS potential can be decomposed into a spin-independent part and a spin-dependent part (here, the presence of an external magnetic field is excluded):

$$V_{KS}(\mathbf{r}) = \bar{V}_{KS}(\mathbf{r}) + \boldsymbol{\beta} \boldsymbol{\Sigma} \cdot \mathbf{B}_{xc}(\mathbf{r}) = V_{ext}(\mathbf{r}) + V_H(\mathbf{r}) + \bar{V}_{xc}(\mathbf{r}) + \boldsymbol{\beta} \boldsymbol{\Sigma} \cdot \mathbf{B}_{xc}(\mathbf{r})$$

that, in turn, splits up into an external part, a Hartree term, and terms containing the spin-averaged and spin-dependent part of the exchange-correlation potential. The KS potential is given as a functional of the particle and spin magnetization densities

$$n(\mathbf{r}) = \frac{1}{2} \sum_k^{occ} \phi_k^\dagger(\mathbf{r}) \phi_k(\mathbf{r}) + \text{c.c.}, \quad (4)$$

$$\mathbf{m}(\mathbf{r}) = \frac{1}{2} \sum_k^{occ} \phi_k^\dagger(\mathbf{r}) \boldsymbol{\beta} \boldsymbol{\Sigma} \phi_k(\mathbf{r}) + \text{c.c.} \quad (5)$$

For the sake of convenience, from now on we restrict ourselves to the case $\mathbf{B}_{xc} = B_{xc,z} \mathbf{e}_z \equiv B_{xc} \mathbf{e}_z$ and a magnetization density which is collinear to \mathbf{B}_{xc} , i.e., $\mathbf{m} = m_z \mathbf{e}_z \equiv m \mathbf{e}_z$ such that the KS potential takes the form

$$V_{KS}(\mathbf{r}) = \bar{V}_{KS}(\mathbf{r}) + \boldsymbol{\beta} \Sigma_z B_{xc}(\mathbf{r}). \quad (6)$$

In what follows, we will derive the ROPM equations starting from Eq. (1) and recast it in different forms to make contact to other formulations found in the literature^{4,6,10,28} and to set the framework for a numerical solution of the problem.

Starting from the definition of the KS potentials

$$\bar{V}_{xc}(\mathbf{r}) = \frac{\delta E_{xc}[n, m]}{\delta n(\mathbf{r})}, \quad B_{xc}(\mathbf{r}) = \frac{\delta E_{xc}[n, m]}{\delta m(\mathbf{r})} \quad (7)$$

and applying the chain rule for functional derivatives, one obtains (neglecting the eigenvalue dependence of E_{xc})

$$\bar{V}_{xc}(\mathbf{r}) = \int d^3r' d^3r'' \left(\sum_k \frac{\delta \phi_k^\dagger(\mathbf{r}')}{\delta \bar{V}_{KS}(\mathbf{r}'')} \frac{\delta E_{xc}[n, m]}{\delta \phi_k^\dagger(\mathbf{r}')} + \text{c.c.} \right) \frac{\delta \bar{V}_{KS}(\mathbf{r}'')}{\delta n(\mathbf{r})} + \left(\sum_k \frac{\delta \phi_k^\dagger(\mathbf{r}')}{\delta B_{xc}(\mathbf{r}'')} \frac{\delta E_{xc}[n, m]}{\delta \phi_k^\dagger(\mathbf{r}')} + \text{c.c.} \right) \frac{\delta B_{xc}(\mathbf{r}'')}{\delta n(\mathbf{r})}. \quad (8)$$

Here, the functions $\frac{\delta \bar{V}_{KS}(\mathbf{r}'')}{\delta n(\mathbf{r})} = (\chi^{-1}(\mathbf{r}'', \mathbf{r}))_{nn}$ and $\frac{\delta B_{xc}(\mathbf{r}'')}{\delta n(\mathbf{r})} = (\chi^{-1}(\mathbf{r}'', \mathbf{r}))_{mn}$ are the charge-charge (n, n) and magnetization-charge (m, n) elements of the inverse of the static noninteracting KS-response functions (see Sec. II F). Proceeding likewise for the term in B_{xc} [Eq. (7)] and combining the results, one obtains

$$\begin{pmatrix} \bar{V}_{xc}(\mathbf{r}) \\ B_{xc}(\mathbf{r}) \end{pmatrix}^T = \int d^3r' d^3r'' \left(\begin{array}{c} \sum_k \frac{\delta\phi_k^\dagger(\mathbf{r}')}{\delta\bar{V}_{KS}(\mathbf{r}'')} \frac{\delta E_{xc}[n,m]}{\delta\phi_k^\dagger(\mathbf{r}')} + \text{c.c.} \\ \sum_k \frac{\delta\phi_k^\dagger(\mathbf{r}')}{\delta B_{xc}(\mathbf{r}'')} \frac{\delta E_{xc}[n,m]}{\delta\phi_k^\dagger(\mathbf{r}')} + \text{c.c.} \end{array} \right)^T \begin{pmatrix} (\chi^{-1}(\mathbf{r}'', \mathbf{r}))_{nn} & (\chi^{-1}(\mathbf{r}'', \mathbf{r}))_{nm} \\ (\chi^{-1}(\mathbf{r}'', \mathbf{r}))_{mn} & (\chi^{-1}(\mathbf{r}'', \mathbf{r}))_{mm} \end{pmatrix}. \quad (9)$$

Multiplying this equation from the right by $\chi(\mathbf{r}, \mathbf{r}'')$ that combines the four response functions as done in the right hand side of Eq. (9), integrating over \mathbf{r} , and using

$$\sum_{\mu=n,m} \int d^3r' (\chi^{-1}(\mathbf{r}'', \mathbf{r}))_{\nu\mu} \chi_{\mu\sigma}(\mathbf{r}, \mathbf{r}'') = \delta_{\nu\sigma} \delta(\mathbf{r}'' - \mathbf{r}'') \quad (10)$$

leads to

$$\int d^3r' \begin{pmatrix} \bar{V}_{xc}(\mathbf{r}') \\ B_{xc}(\mathbf{r}') \end{pmatrix}^T \chi(\mathbf{r}', \mathbf{r}) = \begin{pmatrix} I_V(\mathbf{r}) \\ I_B(\mathbf{r}) \end{pmatrix}^T \quad (11)$$

as an integral equation for the KS potentials \bar{V}_{xc} and B_{xc} . Here, we have used the abbreviations

$$I_V(\mathbf{r}) = \int d^3r' \sum_k \frac{\delta\phi_k^\dagger(\mathbf{r}')}{\delta\bar{V}_{KS}(\mathbf{r})} \frac{\delta E_{xc}[n,m]}{\delta\phi_k^\dagger(\mathbf{r}')} + \text{c.c.}, \quad (12)$$

$$\int d^3r' \begin{pmatrix} \bar{V}_{xc}(\mathbf{r}') \\ B_{xc}(\mathbf{r}') \end{pmatrix}^T \begin{pmatrix} \chi_{nn}(\mathbf{r}, \mathbf{r}') & \chi_{nm}(\mathbf{r}, \mathbf{r}') \\ \chi_{nm}(\mathbf{r}, \mathbf{r}') & \chi_{mm}(\mathbf{r}, \mathbf{r}') \end{pmatrix} = \int d^3r' \sum_k \begin{pmatrix} \phi_k^\dagger(\mathbf{r}') G_k(\mathbf{r}, \mathbf{r}') & [\bar{V}_{xc}(\mathbf{r}') + \beta \Sigma_z B_{xc}(\mathbf{r}')] \phi_k(\mathbf{r}') \\ \phi_k^\dagger(\mathbf{r}') \beta \Sigma_z G_k(\mathbf{r}, \mathbf{r}') & [\bar{V}_{xc}(\mathbf{r}') + \beta \Sigma_z B_{xc}(\mathbf{r}')] \phi_k(\mathbf{r}') \end{pmatrix}^T \quad (14)$$

and the right hand side with the use of the Eqs. (28) as

$$\begin{aligned} & \int d^3r' \sum_k \begin{pmatrix} \frac{\delta\phi_k^\dagger(\mathbf{r}')}{\delta\bar{V}_{KS}(\mathbf{r})} \frac{\delta E_{xc}[n,m]}{\delta\phi_k^\dagger(\mathbf{r}')} + \text{c.c.} \\ \frac{\delta\phi_k^\dagger(\mathbf{r}')}{\delta B_{xc}(\mathbf{r})} \frac{\delta E_{xc}[n,m]}{\delta\phi_k^\dagger(\mathbf{r}')} + \text{c.c.} \end{pmatrix}^T \\ &= \int d^3r' \sum_k \begin{pmatrix} \phi_k^\dagger(\mathbf{r}') G_k(\mathbf{r}, \mathbf{r}') \frac{\delta E_{xc}[n,m]}{\delta\phi_k^\dagger(\mathbf{r}')} + \text{c.c.} \\ \phi_k^\dagger(\mathbf{r}') \beta \Sigma_z G_k(\mathbf{r}, \mathbf{r}') \frac{\delta E_{xc}[n,m]}{\delta\phi_k^\dagger(\mathbf{r}')} + \text{c.c.} \end{pmatrix}^T. \end{aligned} \quad (15)$$

Introducing now the orbital shift ψ_k^{sft}

$$I_B(\mathbf{r}) = \int d^3r' \sum_k \frac{\delta\phi_k^\dagger(\mathbf{r}')}{\delta B_{xc}(\mathbf{r})} \frac{\delta E_{xc}[n,m]}{\delta\phi_k^\dagger(\mathbf{r}')} + \text{c.c.} \quad (13)$$

to denote the inhomogeneity of the integral equation (11).

The KS-response function can be expressed in terms of the orbitals ϕ_k (see Sec. II F). The functional derivatives of the orbitals ϕ_k with respect to the KS potentials can be obtained by first order perturbation theory (see Sec. II D). Therefore, if an explicit form for E_{xc} is given, this integral equation can be solved to obtain the potentials \bar{V}_{xc} and B_{xc} .

The potentials $\bar{V}_{xc}(\mathbf{r})$ and $B_{xc}(\mathbf{r})$ as solution of the integral equation (11) are determined up to a constant. They will be fixed using a spin-projected representation (see Sec. III A).

B. Alternative forms of the relativistic optimized potential method equations

Starting from Eq. (11), one can rewrite the left hand side with the use of Eq. (36) as

$$\psi_k^{sft}(\mathbf{r}) = \int d^3r' G_k(\mathbf{r}, \mathbf{r}') \left[(\bar{V}_{xc}(\mathbf{r}') + \beta \Sigma_z B_{xc}(\mathbf{r}')) \phi_k(\mathbf{r}') - \frac{\delta E_{xc}[n,m]}{\delta\phi_k^\dagger(\mathbf{r}')} \right], \quad (16)$$

this can be rewritten as

$$\sum_k^{occ} \phi_k^\dagger(\mathbf{r}) \psi_k^{sft}(\mathbf{r}) + \text{c.c.} = 0, \quad (17)$$

$$\sum_k^{occ} \phi_k^\dagger(\mathbf{r}) \beta \Sigma_z \psi_k^{sft}(\mathbf{r}) + \text{c.c.} = 0. \quad (18)$$

Here, $G_k(\mathbf{r}', \mathbf{r})$ is the Green's function of the Dirac equation (1) projected into the subspace orthogonal to ϕ_k .^{4,18,19} For the spin-dependent potential considered in Eq. (6), its construction is much more involved than in the cases considered in the literature so far. Its construction is given in Ref. 34 and

is briefly outlined in Sec. II E. The orbital shift ψ_k^{ft} has been discussed extensively in nonrelativistic formulations of the OPM.^{6,28,30} It represents the first order change in the wave functions due to the replacement of the orbital-dependent potential $\frac{\delta E_{xc}[n,m]}{\delta \phi_k^\dagger(\mathbf{r})}$ with the common potential $\bar{V}_{xc}(\mathbf{r}) + \beta \Sigma_z B_{xc}(\mathbf{r})$ seen by all electrons. In a nonrelativistic formulation, the counterpart of Eq. (17) has been used by Kümmel and Perdew^{28,29} to construct an iterative scheme to solve the OPM equations, bypassing some problems in the conventional formulation caused by the need to invert response functions. Below we will give a relativistic generalization of this scheme and try to judge its efficiency for open-shell systems from our numerical investigations.

Following earlier ideas of Krieger *et al.*³⁰ and Kreibich *et al.*,³⁵ one can derive yet another explicit form of the ROPM equations, which makes use of the orbital shifts defined in Eq. (16). First, by using Eq. (30), one obtains the following differential equation for the shift:

$$[\mathcal{H}_D - \epsilon_k] \psi_k^{ft}(\mathbf{r}) = - \left[(\bar{V}_{xc}(\mathbf{r}) + \beta \Sigma_z B_{xc}(\mathbf{r})) \phi_k(\mathbf{r}) - \frac{\delta E_{xc}}{\delta \phi_k^\dagger(\mathbf{r})} \right] + [\bar{A}_{xc} - \bar{u}_{xc}] \phi_k(\mathbf{r}), \quad (19)$$

where

$$\bar{A}_{xc} = \int d^3r \phi_k^\dagger(\mathbf{r}) (\bar{V}_{xc}(\mathbf{r}) + \beta \Sigma_z B_{xc}(\mathbf{r})) \phi_k(\mathbf{r}),$$

$$\bar{u}_{xc} = \int d^3r \phi_k^\dagger(\mathbf{r}) \frac{\delta E_{xc}}{\delta \phi_k^\dagger(\mathbf{r})}$$

are the averages of the potentials with respect to the k th orbital. Multiplying Eq. (17) by $\bar{V}_{KS}(\mathbf{r})$ and using Eq. (19), one arrives at

$$\begin{pmatrix} \bar{V}_{xc}(\mathbf{r}) \\ B_{xc}(\mathbf{r}) \end{pmatrix} = \frac{\mathcal{J}^{-1}(\mathbf{r})}{2} \begin{pmatrix} \sum_k \{a_{xc}^V(\mathbf{r}) + [\bar{A}_{xc} - \bar{u}_{xc}] \phi_k^\dagger(\mathbf{r}) \phi_k(\mathbf{r}) + \text{c.c.}\} \\ \sum_k \{a_{xc}^B(\mathbf{r}) + [\bar{A}_{xc} - \bar{u}_{xc}] \phi_k^\dagger(\mathbf{r}) \beta \Sigma_z \phi_k(\mathbf{r}) + \text{c.c.}\} \end{pmatrix}. \quad (25)$$

The last equation represents an exact transformation of the ROPM equation. By omitting the terms in ψ^{ft} in the coefficients a_{xc}^V and a_{xc}^B [Eqs. (21) and (23)], the relativistic KLI (RKLI) approximation is obtained, which has been extensively discussed in the non-spin-polarized relativistic^{10,35} as well as in the nonrelativistic context.^{6,26}

C. Relativistic wave functions

For the solution of Eq. (1) for a given spin-dependent potential, we closely follow the ansatz worked out

$$\begin{aligned} \bar{V}_{xc}(\mathbf{r}) \sum_k \phi_k^\dagger(\mathbf{r}) \phi_k(\mathbf{r}) + B_{xc}(\mathbf{r}) \sum_k \phi_k^\dagger(\mathbf{r}) \beta \Sigma_z \phi_k(\mathbf{r}) + \text{c.c.} \\ = 2\bar{V}_{xc}(\mathbf{r}) n(\mathbf{r}) + 2B_{xc}(\mathbf{r}) m(\mathbf{r}) \\ = \sum_k \{a_{xc}^V(\mathbf{r}) + [\bar{A}_{xc} - \bar{u}_{xc}] \phi_k^\dagger(\mathbf{r}) \phi_k(\mathbf{r}) + \text{c.c.}\}, \quad (20) \end{aligned}$$

where

$$\begin{aligned} a_{xc}^V(\mathbf{r}) = \phi_k^\dagger(\mathbf{r}) \frac{\delta E_{xc}}{\delta \phi_k^\dagger(\mathbf{r})} + \phi_k^\dagger(\mathbf{r}) \left[ic \boldsymbol{\alpha} \cdot \nabla - \frac{c^2}{2} (\beta - 1) \right. \\ \left. - \beta \Sigma_z B_{xc}(\mathbf{r}) + \epsilon_k \right] \psi_k^{ft}(\mathbf{r}) + \text{c.c.} \quad (21) \end{aligned}$$

Likewise, multiplying Eq. (18) by $\bar{V}_{KS}(\mathbf{r})$ leads to

$$\begin{aligned} \bar{V}_{xc}(\mathbf{r}) \sum_k \phi_k^\dagger(\mathbf{r}) \beta \Sigma_z \phi_k(\mathbf{r}) + B_{xc}(\mathbf{r}) \sum_k \phi_k^\dagger(\mathbf{r}) \phi_k(\mathbf{r}) + \text{c.c.} \\ = 2\bar{V}_{xc}(\mathbf{r}) m(\mathbf{r}) + 2B_{xc}(\mathbf{r}) n(\mathbf{r}) = \sum_k \{a_{xc}^B(\mathbf{r}) + [\bar{A}_{xc} \\ - \bar{u}_{xc}] \phi_k^\dagger(\mathbf{r}) \beta \Sigma_z \phi_k(\mathbf{r}) + \text{c.c.}\}, \quad (22) \end{aligned}$$

with

$$\begin{aligned} a_{xc}^B(\mathbf{r}) = \phi_k^\dagger(\mathbf{r}) \beta \Sigma_z \frac{\delta E_{xc}}{\delta \phi_k^\dagger(\mathbf{r})} + \phi_k^\dagger(\mathbf{r}) \beta \Sigma_z \left[ic \boldsymbol{\alpha} \cdot \nabla - \frac{c^2}{2} (\beta - 1) \right. \\ \left. - \beta \Sigma_z B_{xc}(\mathbf{r}) + \epsilon_k \right] \psi_k^{ft}(\mathbf{r}) + \text{c.c.} \quad (23) \end{aligned}$$

Equations (20) and (22) constitute a system of linear equations for the potentials. Defining now the matrix

$$\mathcal{J}(\mathbf{r}) = \begin{pmatrix} n(\mathbf{r}) & m(\mathbf{r}) \\ m(\mathbf{r}) & n(\mathbf{r}) \end{pmatrix}, \quad (24)$$

its solution can be written in the convenient form

before.^{36,37} The solutions of Eq. (1) are expanded into four spinors of the form

$$\phi_k(\mathbf{r}) = \sum_{\Lambda} \begin{pmatrix} g_{\Lambda k}(r) \chi_{\Lambda}(\hat{r}) \\ if_{\Lambda k}(r) \chi_{-\Lambda}(\hat{r}) \end{pmatrix}, \quad (26)$$

where g and f are the radial functions of the large and small components, respectively, and χ_{Λ} are the usual spin-angular functions.³³ The combined quantum number $k = (n\Lambda)$ is used to label the states which can have mixed spin-angular character. Here, n denotes the principal quantum number, Λ

$=(\kappa, \mu)$ is a combined index comprising the spin-orbit and magnetic quantum number. We also use the following notation: $\bar{\Lambda} = (-\kappa - 1, \mu)$ and $-\Lambda = (-\kappa, \mu)$.

Assuming the fields $\bar{V}_{KS}(\mathbf{r})$ and $B_{xc}(\mathbf{r})$ to be spherically symmetric (see below), inserting the expansion (26) into Eq. (1) leads to an infinite set of coupled first order differential equations. The coupling is due to the exchange field B_{xc} . Fortunately, the coupling can be restricted to the coupling of at most two partial waves:³⁸ one having spin-angular character Λ , the other $\bar{\Lambda}$. This leads to two possible cases: For the case (i) $|\mu| = l + \frac{1}{2}$, no $\Lambda - \bar{\Lambda}$ coupling is possible and one is left with the standard set of two coupled radial differential equations. There is no mixing of spin-angular character: $\phi_k = (g_{\Lambda k} \chi_{\Lambda}, i f_{\Lambda k} \chi_{-\Lambda})^T$. For the case (ii) $|\mu| \neq l + \frac{1}{2}$, a set of four coupled differential equations is obtained. The two physical (i.e., normalizable) solutions found in this case (in each of which the coupling is mediated through the same μ) will have mixed spin-angular character and have the following form:

$$\phi_k^{\gamma}(\mathbf{r}) = \begin{pmatrix} g_{\Lambda k}^{\gamma}(r) \chi_{\Lambda}(\hat{r}) \\ i f_{\Lambda k}^{\gamma}(r) \chi_{-\Lambda}(\hat{r}) \end{pmatrix} + \begin{pmatrix} g_{\bar{\Lambda} k}^{\gamma}(r) \chi_{\bar{\Lambda}}(\hat{r}) \\ i f_{\bar{\Lambda} k}^{\gamma}(r) \chi_{-\bar{\Lambda}}(\hat{r}) \end{pmatrix}, \quad (27)$$

where we have introduced for convenience an additional index γ to discern the two solutions.

The physical solutions are found by inward (starting from a large r value) and outward integrations (from nucleus), respectively, starting from the appropriate boundary conditions and matching them at an intermediate mesh point. Let us mention here that in case (ii) care has to be taken to find both solutions $\gamma=1$ and $\gamma=2$.^{36,37} Having found one of the solutions (say, $\gamma=1$), we found it convenient to exchange the weights for the radial components belonging to the Λ and $\bar{\Lambda}$ components, respectively, and use them as starting values for the outward integration when searching for the second solution ($\gamma=2$).

D. Perturbation theory

Given $V_{KS}(\mathbf{r}) = \bar{V}_{KS}(\mathbf{r}) + \beta \Sigma_z B_{xc}(\mathbf{r})$ (here, B_{xc} is the z component of \mathbf{B}_{xc}), first order perturbation theory gives the following for the various functional derivatives occurring in Eqs. (8) and (9):

$$\begin{aligned} \frac{\delta \phi_k(\mathbf{r}')}{\delta \bar{V}_{KS}(\mathbf{r})} &= G_k(\mathbf{r}', \mathbf{r}) \phi_k(\mathbf{r}), \\ \frac{\delta \phi_k^{\dagger}(\mathbf{r}')}{\delta \bar{V}_{KS}(\mathbf{r})} &= \phi_k^{\dagger}(\mathbf{r}) G_k(\mathbf{r}, \mathbf{r}'), \\ \frac{\delta \phi_k(\mathbf{r}')}{\delta B_{xc}(\mathbf{r})} &= G_k(\mathbf{r}', \mathbf{r}) \beta \Sigma_z \phi_k(\mathbf{r}), \\ \frac{\delta \phi_k^{\dagger}(\mathbf{r}')}{\delta B_{xc}(\mathbf{r})} &= \phi_k^{\dagger}(\mathbf{r}) \beta \Sigma_z G_k(\mathbf{r}, \mathbf{r}'), \end{aligned} \quad (28)$$

with the Green's function

$$G_k(\mathbf{r}', \mathbf{r}) = \sum_{i \neq k} \frac{\phi_i(\mathbf{r}') \phi_i^{\dagger}(\mathbf{r})}{\epsilon_k - \epsilon_i} = G_k^{\dagger}(\mathbf{r}, \mathbf{r}'), \quad (29)$$

whose construction is given in Sec. II E. By construction, it is orthogonal to the state $\phi_k(\mathbf{r})$.

E. Construction of the orthogonal Green's function

The Green's function $G_k(\mathbf{r}, \mathbf{r}')$ of the Dirac Eq. (1) projected into the subspace orthogonal to ϕ_k is defined as the solution of the following differential equation:

$$(\epsilon_k - \mathcal{H}_D) G_k(\mathbf{r}, \mathbf{r}') = \delta(\mathbf{r} - \mathbf{r}') - \phi_k(\mathbf{r}) \phi_k^{\dagger}(\mathbf{r}'). \quad (30)$$

For case (i) of having no $\Lambda - \bar{\Lambda}$ coupling present, one is left with a set of two coupled first order differential equations in g and f . The Green's function is built from the two independent solutions of this system, where as one of them the physical solution ϕ_k is taken and a second (non-normalizable) solution ψ_k is constructed following the procedure of Talman and co-workers.^{4,19} It is given as

$$\begin{aligned} G_k(\mathbf{r}, \mathbf{r}') &= \Gamma_k(\mathbf{r}, \mathbf{r}') - \Psi_k(\mathbf{r}) \phi_k^{\dagger}(\mathbf{r}') - \phi_k(\mathbf{r}) \Psi_k^{\dagger}(\mathbf{r}') \\ &\quad + K_k \phi_k(\mathbf{r}) \phi_k^{\dagger}(\mathbf{r}'). \end{aligned} \quad (31)$$

Here, $\Gamma(\mathbf{r}, \mathbf{r}')$ is the Green's function for the Hamiltonian in Eq. (2) constructed as

$$\Gamma_k(\mathbf{r}, \mathbf{r}') = \phi_k(\mathbf{r}) \psi_k^{\dagger}(\mathbf{r}') \Theta(r - r') + \psi_k(\mathbf{r}) \phi_k^{\dagger}(\mathbf{r}') \Theta(r' - r), \quad (32)$$

fulfilling the equation $\mathcal{H}_D \Gamma_k(\mathbf{r}, \mathbf{r}') = \delta(\mathbf{r} - \mathbf{r}')$. The auxiliary function Ψ_k is given by

$$\Psi_k(\mathbf{r}) = \int d^3 r' \Gamma_k(\mathbf{r}, \mathbf{r}') \phi_k(\mathbf{r}'), \quad (33)$$

and $K_k = \int d^3 r' \phi_k^{\dagger}(\mathbf{r}') \Psi_k(\mathbf{r})$ is an overlap integral.

For case (ii) with $\Lambda - \bar{\Lambda}$ coupling present, the construction of G_k is much more involved (specific details on the construction of the orthogonal Green's function in this case will be given in a subsequent publication³⁴ by the authors). A set of four coupled differential equations is obtained, whose linear independent solutions shall be denoted as ϕ_k (the normalizable solution), ψ_k , $\tilde{\phi}_k$, and $\tilde{\psi}_k$, each of which has the form (27). This leads to

$$\begin{aligned} \Gamma_k(\mathbf{r}, \mathbf{r}') &= \phi_k(\mathbf{r}) \psi_k^{\dagger}(\mathbf{r}') \Theta(r - r') + \psi_k(\mathbf{r}) \phi_k^{\dagger}(\mathbf{r}') \Theta(r' - r) \\ &\quad + \tilde{\phi}_k(\mathbf{r}) \tilde{\psi}_k^{\dagger}(\mathbf{r}') \Theta(r - r') + \tilde{\psi}_k(\mathbf{r}) \tilde{\phi}_k^{\dagger}(\mathbf{r}') \Theta(r' - r). \end{aligned} \quad (34)$$

Using this, the orthogonal Green's function $G_k(\mathbf{r}, \mathbf{r}')$ has the form of Eq. (31) with Γ_k replaced by the one given in Eq. (34).

F. Response functions

The KS-response functions occurring in Eq. (8) and the following are defined as

$$\chi(\mathbf{r}, \mathbf{r}') = \begin{pmatrix} \frac{\delta n(\mathbf{r})}{\delta \bar{V}_{KS}(\mathbf{r}')} & \frac{\delta n(\mathbf{r})}{\delta B_{xc}(\mathbf{r}')} \\ \frac{\delta m(\mathbf{r})}{\delta \bar{V}_{KS}(\mathbf{r}')} & \frac{\delta m(\mathbf{r})}{\delta B_{xc}(\mathbf{r}')} \end{pmatrix} = \begin{pmatrix} \chi_{nn}(\mathbf{r}, \mathbf{r}') & \chi_{nm}(\mathbf{r}, \mathbf{r}') \\ \chi_{mn}(\mathbf{r}, \mathbf{r}') & \chi_{mm}(\mathbf{r}, \mathbf{r}') \end{pmatrix}. \quad (35)$$

Using the operators $O^\nu \in \{\mathbb{1}_4, \beta \Sigma_z\}$, where $\nu=n$ and m denotes the association with the charge and magnetization densities, respectively, the static KS-response functions can be written as

$$\chi_{\mu\nu}(\mathbf{r}', \mathbf{r}) = \sum_k^{occ} \phi_k^\dagger(\mathbf{r}') O^\mu G_k(\mathbf{r}', \mathbf{r}) O^\nu \phi_k(\mathbf{r}). \quad (36)$$

They obey the symmetry property

$$\chi_{\mu\nu}(\mathbf{r}', \mathbf{r}) = \chi_{\nu\mu}^\dagger(\mathbf{r}, \mathbf{r}'). \quad (37)$$

For $\mu=\nu=n$, one immediately obtains, with the help of Eq. (29) and $\langle \phi_i | \phi_j \rangle = \delta_{ij}$,

$$\int d^3r \chi_{nn}(\mathbf{r}, \mathbf{r}') = \int d^3r' \chi_{nn}(\mathbf{r}, \mathbf{r}') = 0. \quad (38)$$

As mentioned above, we restrict the formulation to the collinear case with $\mathbf{m} = m \mathbf{e}_z$ and $\mathbf{B}_{xc} = B_{xc} \mathbf{e}_z$. For the more general case, the response matrix in Eq. (35) has to be extended to a 4×4 block that would include entries corresponding to the components m_x, m_y and B_{xc}^x, B_{xc}^y , respectively.

III. IMPLEMENTATION

For an implementation of the above scheme, we use the relativistic exact exchange, which is given as an explicit functional of the orbitals

$$E_x = - \sum_{kl}^{occ} \int d^3r \int d^3r' \frac{\phi_k^\dagger(\mathbf{r}) \phi_l(\mathbf{r}) \phi_l^\dagger(\mathbf{r}') \phi_k(\mathbf{r}')}{|\mathbf{r} - \mathbf{r}'|}. \quad (39)$$

We assume a spherically symmetric KS potential, i.e., $V_{KS}(\mathbf{r}) = V_{KS}(r)$, which implies the same property for \bar{V}_{xc} and B_{xc} . In the self-consistency procedures described below, spherical averages of the charge and magnetization densities will be used. Spherical averages of other quantities will be indicated at the appropriate places. The averaging procedures will automatically imply that the obtained potentials will also be spherically symmetric. The orbitals, response functions, etc., are computed on a logarithmic radial mesh.

The asymptotic boundary conditions are enforced by fixing the potentials using $V_x^\pm(r) \xrightarrow{r \rightarrow \infty} -\frac{2}{r}$ in a spin-projected (see Sec. III A) representation.

The boundary conditions for the wave functions for the outward integration are found by a power series expansion of the potentials inserted into the respective radial Dirac equations.^{36,37} The boundary condition for the inward integration are obtained likewise.

A. Direct solution of the integral relativistic optimized potential method equation

The conventional way of solving the (R)OPM equations proceeds by discretization of the Fredholm-type integral equation (11) on a mesh and subsequent inversion of the response function. The problem to tackle here is that the response functions will decay rapidly for large r and r' , which leads to numerical instabilities in the numerical inversion procedure. This needs a sensitive handling of the cut radii used to present the radial wave functions and all other related functions. An additional problem encountered here is the spin polarization of the system. In the nonrelativistic formalism, both spin channels are treated separately.^{22,26} Usually the decay of the highest lying orbitals in the different spin channels will be used as an indicator to determine the cut radii. In the relativistic formulation, spin is not a good quantum number anymore. However, the highest occupied orbitals, in general, have nearly pure spin character. Using the corresponding projection operators $\mathcal{P}^\pm = \frac{1}{2}(1 \pm \beta \Sigma_z)$, a spin-projected representation of the potentials, the response function and inhomogeneities can be obtained. Defining

$$\chi(\mathbf{r}, \mathbf{r}')_{\pm\pm} = \frac{1}{4} \sum_k^{occ} \phi_k^\dagger(\mathbf{r}') \mathcal{P}^\pm G_k(\mathbf{r}', \mathbf{r}) \mathcal{P}^\pm \phi_k(\mathbf{r}), \quad (40)$$

χ has in this projected representation the following form:

$$\chi(\mathbf{r}, \mathbf{r}') = \begin{pmatrix} \chi_{++}(\mathbf{r}, \mathbf{r}') & \chi_{+-}(\mathbf{r}, \mathbf{r}') \\ \chi_{-+}(\mathbf{r}, \mathbf{r}') & \chi_{--}(\mathbf{r}, \mathbf{r}') \end{pmatrix}. \quad (41)$$

The inhomogeneities are transformed as

$$I_\pm(\mathbf{r}) = \frac{1}{2} [I_V(\mathbf{r}) \pm I_B(\mathbf{r})], \quad (42)$$

where the spin-projected potentials $V_x^\pm(\mathbf{r}) = \bar{V}_x(\mathbf{r}) \pm B_x(\mathbf{r})$ have been used. The inversion of the equations can now be done by partitioning the χ matrix, introducing the appropriate cut radii in the up- and down-projected channels. For both the inhomogeneities and the response functions, spherical averages are performed.

B. Using the alternative relativistic optimized potential method equations

The alternative set of ROPM equations (25) contains the potentials in an implicit form and is solved iteratively. Starting with a guess for the potentials \bar{V}_x and B_x on the right hand side, new potentials are obtained, which, in turn, again are used to obtain a new set, and this procedure is repeated until self-consistency is reached. Starting with spherically symmetric potentials and performing the spherical average on Eqs. (20) and (22) implies taking a spherical average of the charge and magnetization densities. Note that the spherical averages of the terms in Eqs. (21) and (23) are taken at the very end of the manipulation, i.e., the orbitals are always used in the full expanded form. The KLI approximation has been obtained by neglecting the orbital shift term in Eq. (25).

C. Iterative construction

An iterative construction for the non-spin-polarized non-relativistic case has been worked out by Kümmel and Perdew.²⁸ Here, we give a generalization to the relativistic spin-polarized case of this approach. Regarding the quantities

$$S_n(\mathbf{r}) = \sum_k^{occ} \phi_k^\dagger(\mathbf{r}) \psi_k^{st}(\mathbf{r}) + c.c., \quad (43)$$

$$S_m(\mathbf{r}) = \sum_k^{occ} \phi_k^\dagger(\mathbf{r}) \beta \Sigma_z \psi_k^{st}(\mathbf{r}) + c.c. \quad (44)$$

as residuals for the nonconverged problem, the goal is to modify the potentials such that, finally, the recast OPM equations (17) and (18) are fulfilled. Further analysis shows that a good guess of how to modify the potentials is given as

$$\bar{V}_x^{new}(\mathbf{r}) = \bar{V}_x^{old}(\mathbf{r}) + c_n S_n(\mathbf{r}), \quad (45)$$

$$B_x^{new}(\mathbf{r}) = B_x^{old}(\mathbf{r}) + c_m S_m(\mathbf{r}). \quad (46)$$

The self-consistency cycle consists of a KS loop in which the new potentials \bar{V}_x^{new} and B_x^{new} are used to obtain new orbitals and orbital shifts by solving the full electronic problem. However, we keep the orbitals fixed for some iterations in an inner loop, updating only the orbital shifts via Eq. (16) and optimizing the residuals Eqs. (43) and (44) using the potentials in Eqs. (45) and (46).

IV. RESULTS AND DISCUSSION

In this section, we report on results for the solution of the ROPM equations in the exact exchange approximation for the exchange-correlation functional. Besides the exact solution, either by inversion of the response function or using the mentioned iterative approach, we also employed the KLI approximation. Whereas the latter approximation leads to a fairly simple iteration scheme, the full ROPM equations turned out to be a numerically delicate matter. The reason for the simplicity of the KLI lies in the fact that there is no need for the construction of the orthogonal Green's function and orbital shifts, nor for the inversion of badly conditioned matrices.

As the solution of the full ROPM problem turned out to be so delicate, reliability of the results was ensured by comparing results from two computer codes which have been developed independently of each other, i.e., the involved routines for calculating relativistic matrix elements, Clebsch-Gordan coefficients, to solve the Dirac equation, for the inversion procedure are coded differently. Tests on various systems gave the same results.

The developed computer codes to solve the ROPM equations were tested first on non-spin-polarized systems and compared to the results of an existing implementation.¹⁹ We obtained virtually exactly the same results—deviations of eigenvalues of the orbitals were in the range of 10^{-6} Ry.

To obtain the spin-averaged and spin-dependent potentials \bar{V}_x and B_x , respectively, the response functions $\chi_{\nu\mu}$ (ν, μ

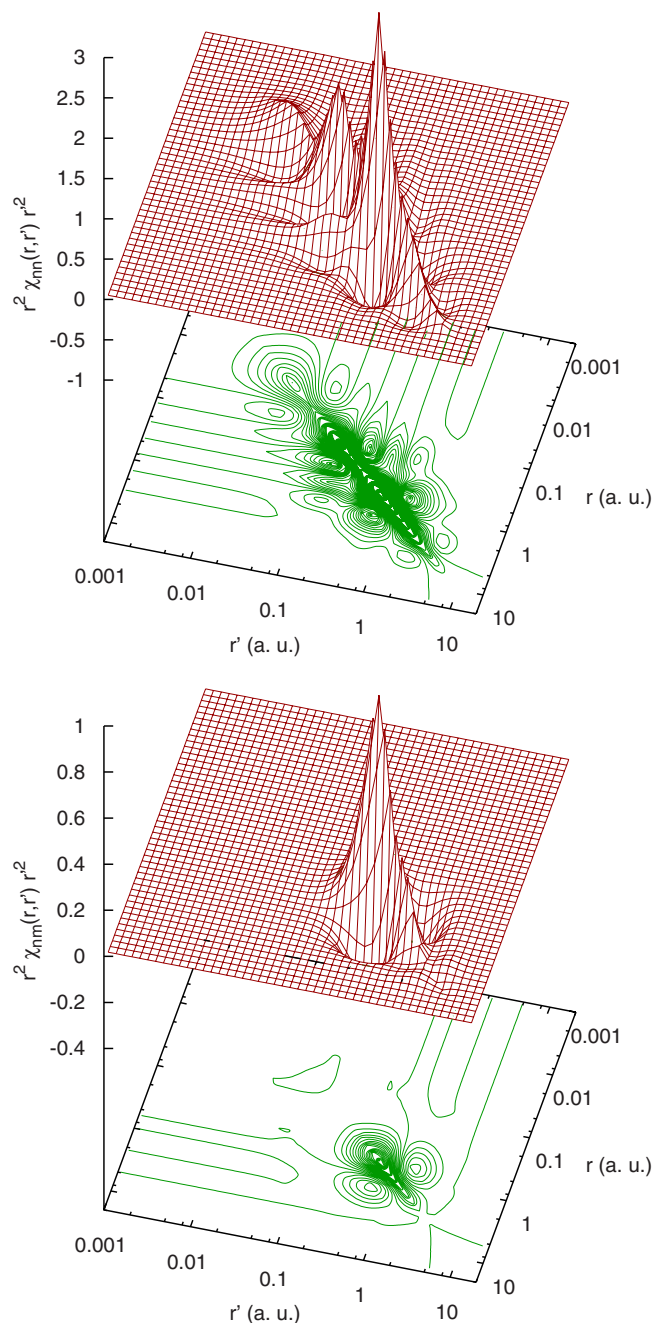


FIG. 1. (Color online) Top: Spherically averaged static charge-charge KS-response function (normalized with the square of the radial coordinates) $r^2 \chi_{nm}(r, r') r'^2$ according to Eq. (36) for the free iron atom dealt with self-consistently using the exact exchange ROPM scheme. Bottom: The charge-magnetization response function for the free iron atom $r^2 \chi_{nm}(r, r') r'^2$.

$\in \{n, m\}$) according to Eq. (35) have to be constructed numerically on an (r, r') grid following the procedure described in Sec. II F using the orthogonal Green's function G_k (see Sec. II E). As an illustrative example, we show in Fig. 1 the normalized response functions associated with the charge- and magnetization densities for the free iron atom. Only two of the four response functions of Eq. (35) are shown, namely, χ_{nm} and χ_{nm} . [Out of the four response func-

TABLE I. Eigenvalues and expectation values for the extension of the orbitals of the free lithium atom. The nonrelativistic OPM results are obtained using a code of one of the authors (Ref. 22).

State	ϵ_m/Ry (ROPM)	ϵ_m/Ry (OPM)	$\langle r \rangle$ (a.u.) (ROPM)
$1s_{-1/2}$	-4.93798	-4.93769	0.57436
$1s_{+1/2}$	-4.10944	-4.10912	0.57396
$2s_{+1/2}$	-0.39261	-0.39257	3.87226

tions $\chi_{\nu\mu}$, the diagonal ones, i.e., the charge-charge (χ_{nn}) and magnetization-magnetization (χ_{mm}) response functions, are very similar. Therefore, only χ_{nn} is shown. The off-diagonal ones, χ_{nm} and χ_{mn} , are related by the symmetry relation Eq. (37).] The charge-charge response function χ_{nn} has a detailed fine structure. The off-diagonal response function χ_{nm} , on the other hand, is less structured; its magnitude, however, is comparable to the diagonal response functions χ_{nn} and χ_{mm} . As is also noticeable, the χ_{nm} response function, in contrast to the χ_{nn} and χ_{mm} response functions, is mainly sizable when r and r' lie in the range of 0.1–2 a.u.

As a first application of the ROPM scheme, results for the ground state of the lithium atom will be discussed. As Li has a nuclear charge $Z=3$, one expects to obtain the solution to be very close to that of a nonrelativistic calculation. That this is indeed the case can be seen in Table I. As the ground state

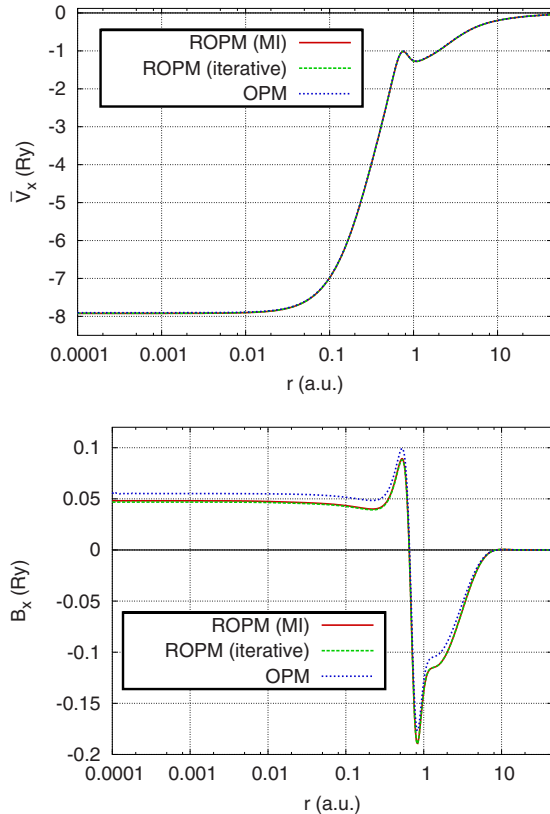


FIG. 2. (Color online) Exchange potentials for the free boron atom. Top: Spin-averaged potentials. Bottom: Exchange fields. Comparison of different solution schemes (matrix inversion vs iterative scheme) and nonrelativistic OPM (Ref. 22).

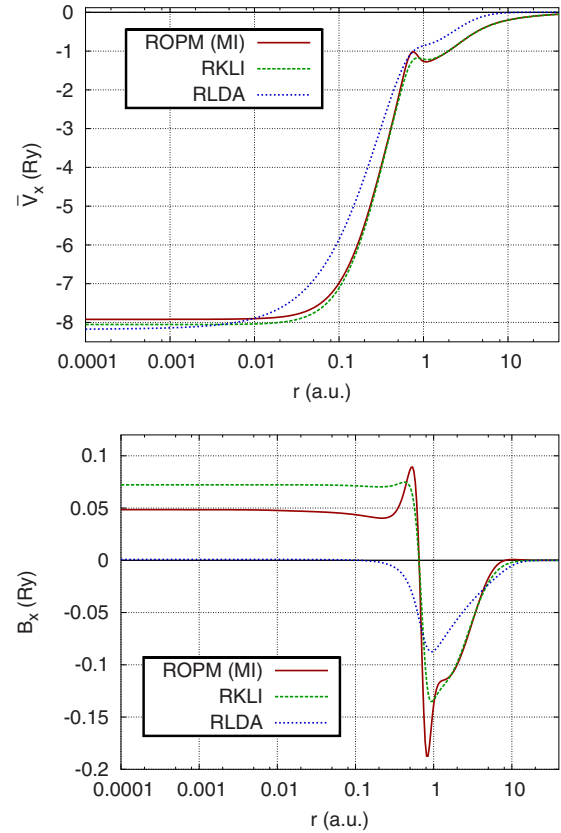


FIG. 3. (Color online) Exchange potentials for the free boron atom, as in Fig. 2. Comparison of different approximation levels of the ROPM (full ROPM vs RKLI) and RLDA.

has only $1s$ and $2s$ states occupied, no relativistic Λ - $\bar{\Lambda}$ coupling within the shells occurs. As typical for the free alkali atoms, the two highest occupied orbitals (projected into the respective spin channels) have a very different decay with increasing radius r , monitored here by the expectation value $\langle r \rangle$.

In Fig. 2, the exchange field of the free boron atom is shown, comparing the full ROPM scheme [matrix inversion (MI)] and ROPM using the iterative scheme to the OPM. Having five electrons and choosing a valence configuration with a p -like state with $|\mu| \neq \frac{3}{2}$, this is the first system in the Periodic Table where the full relativistic Λ - $\bar{\Lambda}$ coupling of the solution within a p shell occurs. As can be seen in Fig. 2, the ROPM spin-averaged potential coincides with that of the OPM. For the exchange field B_x , there are slight deviations between ROPM and OPM. Note that whereas in the nonrelativistic case the p orbitals in one spin channel are degenerate, this degeneracy is broken in the relativistic case. Both full ROPM schemes (MI and iterative construction) give identical results. It turned out, however, that the computational speed of not having to invert response functions was compensated by the very slow convergence of the iterative scheme (typically, some 30 iterations in the MI scheme vs 300 iterations in the iterative scheme). It should be noted that both schemes need the orthogonal Green's function, whose construction is numerically very demanding and turned out

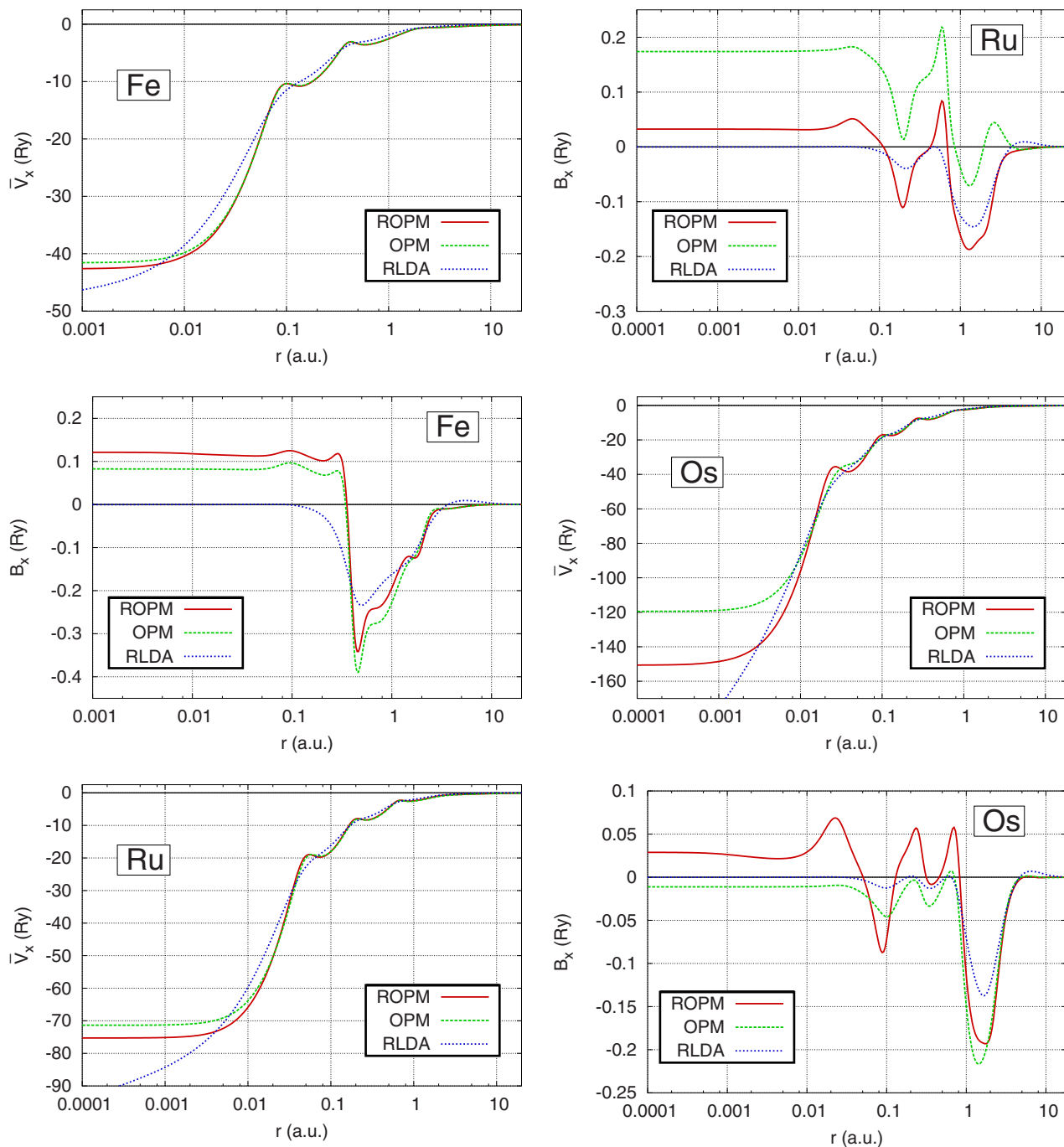


FIG. 4. (Color online) ROPM potentials for free atoms, from top to bottom: iron, ruthenium, and osmium. Left: Spin-averaged potentials, comparing ROPM to nonrelativistic OPM and RLDA. Right: The same for the spin-dependent potentials.

to be much more costly than the matrix inversion. This applies, in particular, for systems with a large number of electrons.

In Fig. 3, the potentials for boron obtained by solving the ROPM equations are compared to those obtained by the simplified RKLI scheme and the relativistic LDA (RLDA). For the RLDA, we used a nonrelativistic exchange functional² $E_x^{nrel}[n_+, n_-]$ of spin-projected densities $n_{\pm}(\mathbf{r}) = \frac{1}{2}[n(\mathbf{r}) \pm m(\mathbf{r})]$. The spin-averaged ROPM and RKLI potentials show the characteristic inner-shell bump at $r \approx 0.6$ a.u.

as compared to the RLDA (Fig. 3), with the strongest formation in the full ROPM. The difference in the structure of the ROPM and RKLI results is even more pronounced in the exchange field B_x (Fig. 3). The RLDA as a local functional shows only an exchange field B_x in the region of local magnetization density $m(r)$ with a nearly vanishing amplitude at the nucleus (see also Ref. 22).

In Fig. 4, the spin-averaged and spin-dependent exchange ROPM potentials for the free iron, ruthenium, and osmium atoms are shown and compared to the nonrelativistic OPM

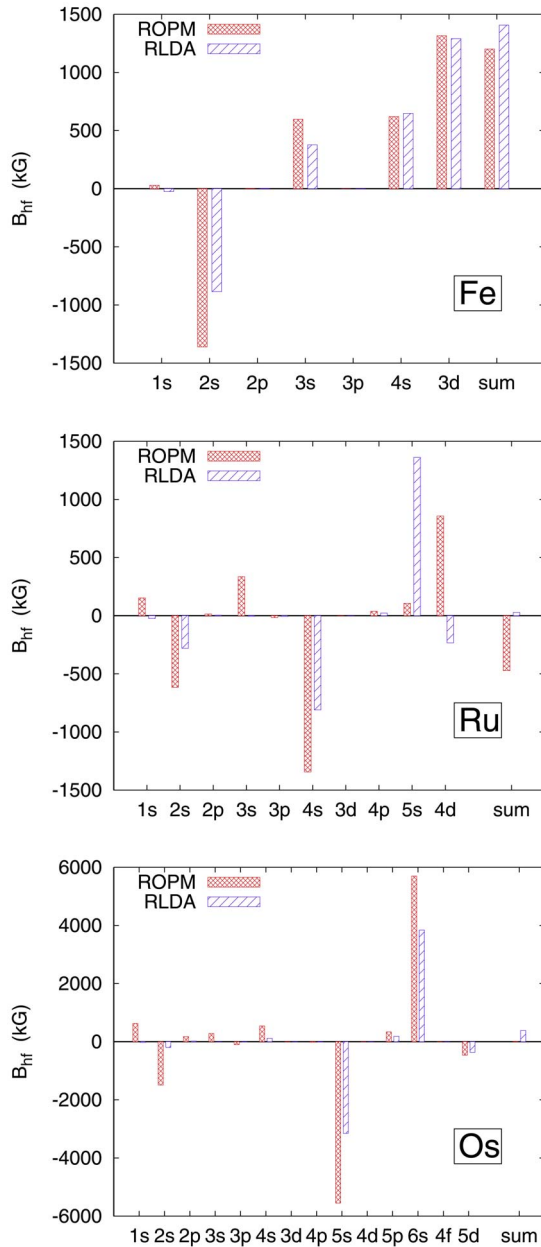


FIG. 5. (Color online) Shell resolved hyperfine fields as obtained by the ROPM scheme compared to the LDA for iron, ruthenium, and osmium.

and RLDA. For all of them, a d^6 configuration has been assumed, i.e., $[\text{Ar}]3d^64s^2$, $[\text{Kr}]4d^6s^2$, and $[\text{Xe}]4f^{14}5d^66s^2$, respectively. In all cases, it turned out that the outermost d orbitals have almost 100% spin polarization. As is apparent, with growing ordering number, the spin-averaged exchange potential in the ROPM gets pushed down at the nucleus when compared to the nonrelativistic OPM. The differences in the spin-dependent exchange do not follow such a systematic trend, but show also distinct changes.

As can be seen in Fig. 4, the spin-dependent ROPM exchange potentials B_x as compared to the LDA have a larger amplitude which also extends to the vicinity of the nucleus. This is a manifestation of the nonlocality of the ROPM po-

tentials. In a local approximation like the LDA, a nonvanishing exchange field can only arise in spatial regions where a finite magnetization is present. This also has an important impact on the hyperfine fields. In Fig. 5, we show the magnitudes of calculated hyperfine fields for the above mentioned free atom cases (Fe, Ru, and Os). A very prominent shortcoming of the local approximation to density functional theory is the overbinding in molecules and solids. Another example is the underestimation of the core polarization contribution to the magnetic hyperfine field due to spin-polarized valence states.³⁶ In fact, Akai and Kotani could more or less remove this problem by the use of the nonrelativistic OPM.³⁹ In Fig. 5, the impact of the use of the ROPM on the hyperfine fields is shown for Fe, Ru, and Os in a shell resolved way. For Fe, the corresponding ROPM and LSDA results differ only quantitatively. Nevertheless, one notes a stronger polarization of the inner core states for the ROPM case. In the case of Ru and Os, the differences are much more pronounced. The reason for this is that the valence states of these elements have a pronounced mixing concerning their spin character due to spin-orbit coupling that sensitively depends on the exchange field B_x . For Fe, on the other hand, the valence states have essentially pure spin character.

V. SUMMARY

We have presented the relativistic optimized potential method formulated in SDFT and implemented the scheme. We have derived several forms of the ROPM equations to give insights into issues connected with the relativistic OPM and to rederive the RKLI approximation.

An implementation of the ROPM was carried out using the relativistic exact exchange functional and making the approximation of spherically symmetric potentials. We presented results of the full ROPM scheme as well as the RKLI approximation for open-shell atoms and compared them to RLDA results.

All results are in full accordance with previous nonrelativistic and unpolarized relativistic studies. Due to the nonlocal character of the ROPM, the resulting exchange potential V_x is, in general, more sharply structured than its LSDA counterpart. For the exchange field B_x , the differences are more pronounced because, for the LSDA case, B_x takes appreciable values only in the spatial regime with an appreciable spin density. Comparing the various schemes to solve the full ROPM problem, we found the same results using the matrix inversion or iterative scheme. Application of the RKLI approximation led—as for corresponding nonrelativistic studies—to potential functions with their peak structure less pronounced when compared to the full ROPM. Comparing the obtained potential functions with their counterpart obtained in a nonrelativistic way, one finds—as to be expected—only slight differences for light elements. With increasing atomic number, differences for the potential V_x show up, in particular, in the nucleus near regime. For the exchange field B_x , on the other hand, differences occur over the whole spatial regime.

The SDFT-ROPM formalism and the related techniques

presented here were applied to free atoms, but can straightforwardly be used to deal with the tightly bound core states in molecules and solids. The corresponding treatment of band states for spin-polarized solids can be achieved by using an appropriate band structure technique that represents the electronic structure in terms of Bloch states.^{40,41} A more general scheme, however, is achieved by representing the electronic Green's function to represent the band states of solids, as has been done by Kotani and Akai⁴² for the non-relativistic case. The corresponding development of the techniques connected with a SDFT-ROPMP for spin-polarized solids is in progress, which—in contrast to previous work—

makes use of a formulation of all functional derivatives and response functions in terms of the Green's function.

ACKNOWLEDGMENTS

Helpful discussions with H. Akai, T. Kotani, as well as with E. K. U. Gross, S. Kurth, N. Helbig, and S. Pittalis are gratefully acknowledged. This work was supported by the Deutsche Forschungsgemeinschaft within the priority program “Moderne und universelle first-principles-Methoden für Mehrelektronensysteme in Chemie und Physik” (SPP 1145).

-
- ¹R. G. Parr and W. Yang, *Density-functional Theory of Atoms and Molecules* (Oxford University Press, New York, 1989).
- ²R. M. Dreizler and E. K. U. Gross, *Density Functional Theory* (Springer-Verlag, Berlin, Heidelberg, 1990).
- ³W. Kohn and L. Sham, Phys. Rev. **140**, A1133 (1965).
- ⁴J. D. Talman and W. F. Shadwick, Phys. Rev. A **14**, 36 (1976).
- ⁵J. P. Perdew and A. Zunger, Phys. Rev. B **23**, 5048 (1981).
- ⁶T. Grabo, T. Kreibich, S. Kurth, and E. K. U. Gross, *Strong Coulomb Correlations and Electronic Structure Calculations: Beyond Local Density Approximations* (Gordon and Breach, New York, 2000), Chap. 1.
- ⁷T. Kotani, Phys. Rev. Lett. **74**, 2989 (1995).
- ⁸T. Kotani and H. Akai, J. Magn. Magn. Mater. **177-181**, 569 (1998).
- ⁹M. Städele, J. A. Majewski, P. Vogl, and A. Görling, Phys. Rev. Lett. **79**, 2089 (1997).
- ¹⁰E. Engel, A. Facco Bonetti, S. Keller, I. Andrejkovics, and R. M. Dreizler, Phys. Rev. A **58**, 964 (1998).
- ¹¹E. Engel and R. M. Dreizler, J. Comput. Chem. **20**, 31 (1999).
- ¹²E. Engel, *A Primer in Density Functional Theory* (Springer, Berlin, 2003), p. 56.
- ¹³M. Lein, J. F. Dobson, and E. K. U. Gross, J. Comput. Chem. **20**, 12 (1999).
- ¹⁴S. Sharma, J. K. Dewhurst, and C. Ambrosch-Draxl, Phys. Rev. Lett. **95**, 136402 (2005).
- ¹⁵S. Rohra and A. Görling, Phys. Rev. Lett. **97**, 013005 (2006).
- ¹⁶S. Sharma, J. K. Dewhurst, C. Ambrosch-Draxl, S. Kurth, N. Helbig, S. Pittalis, S. Shallcross, L. Nordström, and E. K. U. Gross, Phys. Rev. Lett. **98**, 196405 (2007).
- ¹⁷S. Pittalis, S. Kurth, N. Helbig, and E. K. U. Gross, Phys. Rev. A **74**, 062511 (2006).
- ¹⁸J. D. Talman, Comput. Phys. Commun. **54**, 85 (1988).
- ¹⁹B. A. Shadwick, J. D. Talman, and M. R. Norman, Comput. Phys. Commun. **54**, 95 (1989).
- ²⁰J. D. Talman, Phys. Rev. A **72**, 044502 (2005).
- ²¹R. T. Sharp and G. K. Horton, Phys. Rev. **90**, 317 (1953).
- ²²E. Engel and S. H. Vosko, Phys. Rev. A **47**, 2800 (1993).
- ²³G. Vignale and M. Rasolt, Phys. Rev. Lett. **59**, 2360 (1987).
- ²⁴G. Vignale and M. Rasolt, Phys. Rev. B **37**, 10685 (1988).
- ²⁵H. Jiang and E. Engel, J. Chem. Phys. **123**, 224102 (2005).
- ²⁶J. B. Krieger, Y. Li, and G. J. Iafrate, Phys. Rev. A **45**, 101 (1992).
- ²⁷M. Mundt and S. Kümmel, Phys. Rev. A **74**, 022511 (2006).
- ²⁸S. Kümmel and J. P. Perdew, Phys. Rev. Lett. **90**, 043004 (2003).
- ²⁹S. Kümmel and J. P. Perdew, Phys. Rev. B **68**, 035103 (2003).
- ³⁰J. B. Krieger, Y. Li, and G. J. Iafrate, Phys. Rev. A **46**, 5453 (1992).
- ³¹H. Eschrig, *The Fundamentals of Density Functional Theory* (Teubner, Leipzig, 1996).
- ³²M. E. Rose, *Elementary Theory of Angular Momentum* (Wiley, New York, 1961).
- ³³M. E. Rose, *Relativistic Electron Theory* (Wiley, New York, 1961).
- ³⁴E. Engel, D. Ködderitzsch, and H. Ebert (unpublished).
- ³⁵T. Kreibich, E. K. U. Gross, and E. Engel, Phys. Rev. A **57**, 138 (1998).
- ³⁶H. Ebert, J. Phys.: Condens. Matter **1**, 9111 (1989).
- ³⁷E. Engel, T. Auth, and R. M. Dreizler, Phys. Rev. B **64**, 235126 (2001).
- ³⁸R. Feder, F. Rosicky, and B. Ackermann, Z. Phys. B: Condens. Matter **52**, 31 (1983).
- ³⁹H. Akai and T. Kotani, Hyperfine Interact. **120-121**, 3 (1999).
- ⁴⁰H. Ebert, Phys. Rev. B **38**, 9390 (1988).
- ⁴¹B. C. H. Krutzen and F. Springelkamp, J. Phys.: Condens. Matter **1**, 8369 (1989).
- ⁴²T. Kotani and H. Akai, Phys. Rev. B **54**, 16502 (1996).